RESEARCH PAPER

Photocatalytic Degradation of Textile Effluent Using Immobilized Dowex-1×4 Resin as Catalyst Support

Ashutosh Sharma[1], R. C. Meena[2*]

[1] Research Scholar, Department of Chemistry, Jai Narain Vyas University, Jodhpur, India.
Email: ashutosh4u4ever@gmail.com

[2*] Professor, Department of Chemistry, Jai Narain Vyas University, Jodhpur, India (Corresponding Author)

ABSTRACT

The present work investigates the photocatalytic degradation of real textile effluent collected from dyeing units of Jodhpur using an immobilized anion-exchange resin (Dowex-1×4) as catalyst support under UV irradiation. The effluent contained intense coloration primarily from azo dyes such as Metanil Yellow. The catalyst was prepared by impregnating the resin with metal-ion complexes and exposed to a 365 nm UV source. Major operating parameters—initial dye concentration (20–50 mg L^{-1}), catalyst loading (1.00–2.50 g per 100 mL), pH (5–10.5), and light intensity (from 5.4 $mWcm^{-2}$ to 15.5 $mWcm^{-2}$)—were optimized. The degradation followed first-order kinetics, achieving approximately 95% decolorization at 30 mg L^{-1} dye concentration, pH 7.5, 2.00 g catalyst, and 10.5 $mWcm^{-2}$ lamp. The process relies on hydroxyl and superoxide radicals generated through electron–hole separation on the Dowex surface. The study demonstrates the potential of Dowex-supported photocatalysts for efficient, eco-friendly treatment of textile wastewater in arid zones.

Keywords: Photocatalysis; Dowex-1×4 resin; Textile effluent; Metanil Yellow; UV irradiation; Degradation kinetics

How to cite this article: Sharma A, Meena RC. Photocatalytic Degradation of Textile Effluent Using Immobilized Dowex-1×4 Resin as Catalyst Support. Int J Drug Deliv Technol. 2026;16(24s): 993-999. DOI: 10.25258/ijddt.16.24s.119

Source of support: Nil.

Conflict of interest: None

INTRODUCTION

Textile industries release large volumes of colored wastewater rich in synthetic dyes, surfactants, salts, and toxic organics. These effluents exhibit high chemical oxygen demand (COD) and resist biodegradation because many dyes contain azo (–N=N–) linkages and aromatic rings. Conventional treatments—coagulation, chlorination, or adsorption—merely transfer the pollutants from water to sludge without destroying their molecular structure. Therefore, *advanced oxidation processes* (AOPs), particularly *heterogeneous photocatalysis*, have become attractive for complete mineralization of such persistent pollutants [1–4].

Photocatalysis involves the excitation of a semiconductor or photosensitized surface by light energy greater than or equal to its band-gap energy. Upon irradiation, electrons are promoted from the valence band to the conduction band, generating electron–hole pairs (e^-/h^+). These reactive species initiate oxidation–reduction reactions that yield hydroxyl radicals (•OH) and superoxide anions ($O_2^{\bullet -}$). Such radicals non-selectively attack chromophoric bonds, ultimately converting organic contaminants into CO_2 and H_2O [5–7].

Dowex resins are cross-linked polystyrene-based ion-exchange materials possessing uniform porosity, large surface area, and high chemical stability. Their functional quaternary-ammonium groups can immobilize various photoactive species or dye molecules through electrostatic interaction. Compared with powdered TiO_2 or ZnO, immobilized resins offer easy separation, reusability, and reduced turbidity in suspension [8–10]. The Dowex-1×4 resin, having smaller pore diameter than Dowex-1×8, provides faster mass transfer and enhanced adsorption of anionic dyes like Metanil Yellow.

Metanil Yellow ($C_{18}H_{14}N_3NaO_3S$) is a mono-azo dye used widely in textile and paper industries. It imparts a bright yellow-orange color and remains stable under sunlight, acids, and alkalis. Because of its complex aromatic structure, it shows strong resistance to microbial degradation and bio-accumulates in aquatic ecosystems, posing mutagenic and carcinogenic risks [11–13]. Removal of Metanil Yellow from industrial effluent is, therefore, an urgent environmental priority. Recent studies have focused on semiconductor photocatalysts such as TiO_2 [14], ZnO [15], Fe_2O_3 [16], graphitic carbon nitride (g-C_3N_4) [17], and composite materials [18–20]. While these systems show high

activity, their recovery and reuse remain problematic. Polymer-supported catalysts—Dowex, Amberlite, and Nafion—have gained attention for fixed-bed reactor applications [21–26]. Immobilized Dowex–metal oxide hybrids have demonstrated degradation efficiencies of 85–96% for azo dyes within 60 minutes under UV or solar irradiation [27–29].

The textile effluents generated in Jodhpur, Rajasthan, exhibit high coloration, alkalinity, and residual heavy metals. Owing to water scarcity in arid regions, efficient wastewater recycling is essential. The present study aims to evaluate a *Dowex-1×4-supported photocatalytic system* for degrading textile effluent under UV light. The immobilized resin facilitates adsorption–photodegradation synergy, enhances radical formation, and allows convenient recovery for reuse. The work compares degradation behavior across varying operational parameters and establishes kinetic as well as mechanistic insights. The objectives of the present study are-

1. To study the physicochemical characteristics of textile effluent collected from Jodhpur industrial area.
2. To evaluate the effect of operating parameters—initial concentration, pH, catalyst loading, and light intensity—on degradation efficiency.
3. To determine the kinetic model and rate constant of the photocatalytic process.
4. To propose the mechanism of photodegradation and assess its environmental applicability.

MATERIALS AND METHODS

Chemicals and Reagents: All reagents used were of analytical grade. The anion exchange resin **Dowex-1×4 (Cl^- form)** was procured from Sigma–Aldrich and used without further purification. **Metanil Yellow dye** ($C_{18}H_{14}N_3NaO_3S$) was obtained from Merck India and served as a model compound representing the major chromophore in real textile effluent. Sodium hydroxide, hydrochloric acid, potassium dichromate, ferrous ammonium sulfate, and other analytical reagents were used for COD, BOD, and colorimetric analyses as per *APHA (2017)* standard methods.

Collection of Textile Effluent: Real effluent samples were collected from the outlet of a dyeing unit located in the **Basni Industrial Area, Jodhpur**, where reactive and azo dyes are extensively used for cotton fabrics. Samples were taken in pre-cleaned polyethylene containers, filtered through Whatman No. 42 paper, and stored at 4°C before use. The initial color of the effluent was deep orange due to the presence of **Metanil Yellow** and other azo compounds.

Characterization of Effluent: Physicochemical parameters such as pH, conductivity, total dissolved solids (TDS), chemical oxygen demand (COD), biological oxygen demand (BOD), and color intensity were determined before and after photocatalytic treatment. Color removal was monitored spectrophotometrically at 430 nm using a UV–Visible spectrophotometer (Shimadzu UV-1800).

Preparation of Photocatalyst: The photocatalyst was synthesized using Dowex-1×4 resin (20–50 mesh) and methylene blue hydrate. For immobilization, a 1/100 M methylene blue hydrate solution was first prepared in distilled water. The required amount of Dowex-1×4 resin was then introduced into this dye solution, and the mixture was shaken thoroughly to ensure proper interaction between the resin beads and the dye. The suspension was left undisturbed for about 24 hours in a dark environment to allow complete binding of the dye onto the resin surface. After the immobilization period, the resin containing the adsorbed dye was separated by filtration. The collected resin was subsequently rinsed two to three times with double-distilled water to eliminate any excess or unbound dye. The cleaned, dye-loaded resin obtained after washing served as the immobilized photocatalyst for further experiments.

Photocatalytic Reactor Setup: Photocatalytic degradation studies were carried out in a 250-mL borosilicate glass reactor fitted with an immersed 365 nm UV lamp (200 W) placed vertically at the centre and maintained at a constant distance from the catalyst surface. An aluminium reflector was installed around the lamp to minimise radiation losses and ensure maximum UV exposure within the reactor. Under UV illumination, the photocatalytic system operates by generating highly reactive oxygen species and promoting electron excitation, which subsequently interact with dye molecules, leading to their oxidative breakdown. Continuous magnetic stirring was employed to maintain a homogeneous dispersion of the effluent throughout the reaction period. For all the experimental runs, the distance between the UV light source and the reaction interface was kept constant at 6 cm to maintain uniform irradiation conditions.

Experimental Procedure: For each experimental trial, 100 mL of textile wastewater containing the required concentration of Metanil Yellow was introduced into the reactor. The solution pH was adjusted to the target value using 0.1 N HCl or 0.1 N NaOH, depending on the requirement. A catalyst film

equivalent to 0.25 g of immobilized material was affixed to the inner surface of the reactor. Before irradiation, the mixture was stirred magnetically in complete darkness for 30 minutes to allow the system to reach adsorption–desorption equilibrium between the dye molecules and the catalyst. After the equilibration period, the UV lamp was turned on to begin the photocatalytic degradation reaction.

At predetermined intervals (0, 10, 20, 30, 40, 50, …… and 210 minutes), 5 mL aliquots were withdrawn, centrifuged, and analyzed for residual dye concentration by recording absorbance at 430 nm.

Optimization of Parameters: To determine the optimum degradation conditions, several sets of experiments were conducted by varying one parameter at a time while keeping others constant:

- **Initial dye concentration:** 20, 30, 40 and 50 mg L^{-1}
- **Catalyst loading:** 1.00, 1.50, 2.00, 2.50 g
- **pH:** 5, 7.5 and 10.5
- **Light intensity:** 5.4 $mWcm^{-2}$, 10.5 $mWcm^{-2}$ and 15.5 $mWcm^{-2}$

The percentage degradation was calculated using:

$$\text{Degradation } (\%) = \frac{A_0 - A_t}{A_0} \times 100$$

where A_0 and A_t are the initial and instar

Kinetic Analysis: The kinetics of dye degradation followed a **first-order model**:

$$\ln\left(\frac{a}{a-x}\right) = kt$$

Where a represents the initial concentration of the reactant at time $t = 0$. $a - x$ represents the concentration of the reactant remaining at time t. k is the rate constant (min^{-1}) for the reaction. Plots of ln (a/a-x) versus time were constructed to determine k. All experiment were repeated twice, and average values were considered for accuracy.

Analytical Techniques:

- **UV–Vis spectroscopy:** To monitor dye decolorization.
- **FTIR analysis:** To identify structural changes in functional groups after degradation.
- **COD & BOD tests:** To confirm mineralization.
- **pH and conductivity measurements:** To assess ionic variation before and after treatment.

Reusability Test: The used Dowex-1×4 catalytic film was washed with distilled water, dried, and reused for five consecutive cycles. The activity decline, if any, was recorded and expressed as residual efficiency (%). Less than 10% loss in performance after five cycles was considered acceptable for practical application.

RESULTS AND DISCUSSION

Physicochemical Characteristics of Textile Effluent:

Table 1: The Physicochemical Characteristics of the collected effluent

Parameter	Unit	Before Treatment	After Photocatalysis
pH	–	9.2	7.1
Color (Abs at 430 nm)	–	1.38	0.06
COD	mg L^{-1}	785	62
BOD	mg L^{-1}	220	35
Conductivity	µS cm^{-1}	1420	915
TDS	mg L^{-1}	1030	640

The effluent showed strong alkalinity and intense orange coloration due to the presence of azo dyes such as Metanil Yellow. After photocatalytic treatment under UV light with Dowex-1×4 catalyst, substantial decreases were observed in color, COD, and BOD values, confirming efficient degradation and mineralization.

Effect of Initial Dye Concentration: The degradation efficiency decreased with increasing dye concentration (Table 2). At 20 mg L^{-1}, almost 97% color removal was achieved, whereas at 50 mg L^{-1}, efficiency dropped to 68%. Higher concentrations cause light-screening effects, limiting photon penetration and active radical generation.

Table 2: Effect of Initial Dye Concentration

Dye Concentration (mg L^{-1})	% Degradation
20	97
30	95
40	89
50	78

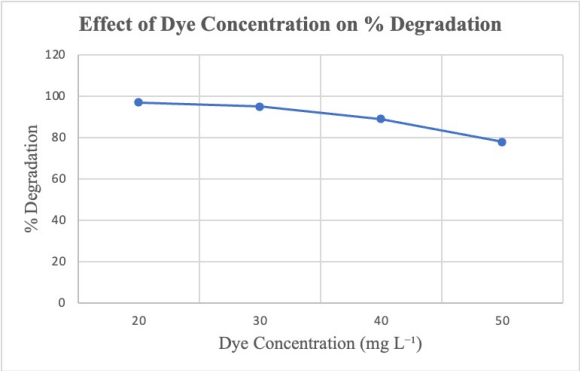

Figure 1: Effect of Initial Dye Concentration

At low dye concentration, all dye molecules adsorb effectively on active sites and undergo radical oxidation. Beyond 40 mg L^{-1}, the surface becomes saturated, and the UV absorption by dye molecules themselves reduces the photon flux reaching the catalyst.

Effect of Catalyst Loading: The effect of catalyst amount on degradation was studied using 1.00–2.50 g Dowex-1×4 (Figure 2). The rate of degradation increased with catalyst loading up to 2.00 g, achieving maximum 95% decolorization, but further increase caused slight decline due to excess scattering and turbidity in the reactor medium.

Table 3: Effect of Catalyst Loading

Catalyst Loading (g)	% Degradation
1.00	68
1.50	82
2.00	95
2.50	87

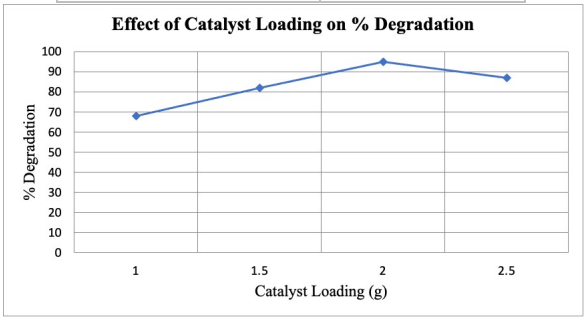

Figure 2: Effect of Catalyst Loading

More catalyst provides more active sites for dye adsorption and radical formation. However, excessive catalyst reduces light transmission and promotes recombination of charge carriers, lowering efficiency. Hence, 2.00 g per 100 mL effluent was taken as optimal.

Effect of pH: The pH of the solution significantly affects both the surface charge of the catalyst and the ionization of the dye molecules. Results (Table 4) revealed that maximum degradation occurred at **neutral pH (≈7.5)**.

Table 4: Effect of pH

pH	% Degradation
5	72
7.5	95
10.5	69

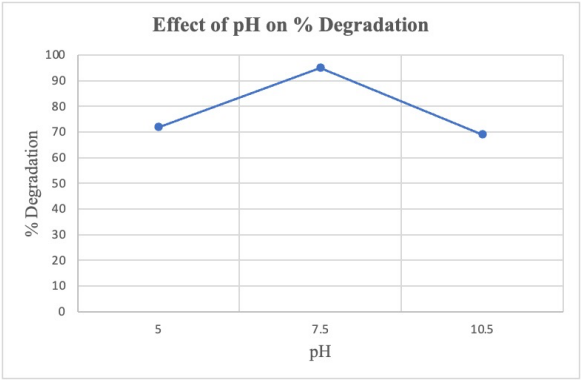

Figure 3: Effect of pH

At low pH, competition between H^+ ions and cationic dye species suppresses adsorption, while at high pH, the excess of OH^- leads to recombination of photogenerated holes. Neutral pH favors stable radical generation and optimum adsorption, consistent with other UV-AOP studies [30–32].

Effect of Light Intensity: Variation of UV lamp power from 5.4 $mWcm^{-2}$ to15.5 $mWcm^{-2}W$ showed a direct relationship between light intensity and degradation rate up to 10.5 $mWcm^{-2}$ (Table 5). Beyond this, the efficiency plateaued, indicating a photon flux saturation limit.

Table 5: Effect of Light Intensity

Light Intensity ($mWcm^{-2}$)	% Degradation
5.4	70
10.5	95
15.5	90

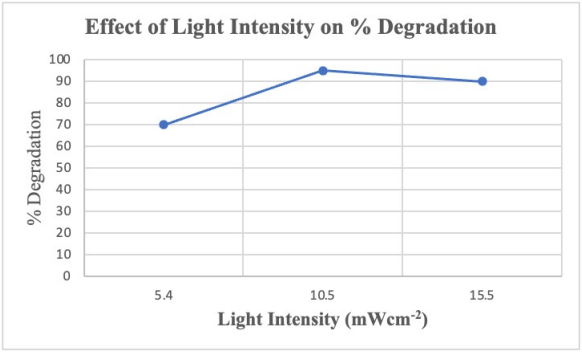

Figure 4: Effect of Light Intensity

The increase in light intensity enhances excitation of the catalyst and radical generation. Above 10.5 $mWcm^{-2}$, recombination dominates due to high carrier density, hence no further improvement occurs.

Kinetic Study: The reaction kinetics followed a first-order model, confirmed by linear plots of ln(a/a-x) versus time ($R^2 > 0.98$). The apparent rate constant **k =**

0.046 min^{-1} at optimum conditions (30 mg L^{-1} dye, pH 7.5, 2.50 g catalyst, 10.5 mWcm^{-2} lamp). Figure 5 shows the kinetic linearization curve.

Equation:

$$\ln\left(\frac{a}{a-x}\right) = kt$$

Table 6: Kinetic Data for Photocatalytic Degradation Showing ln(a/a-x) Variation with Time

Time (min)	ln(a/a-x)
0	0.00
10	0.45
20	0.92
30	1.38
40	1.95
50	2.31
60	2.73

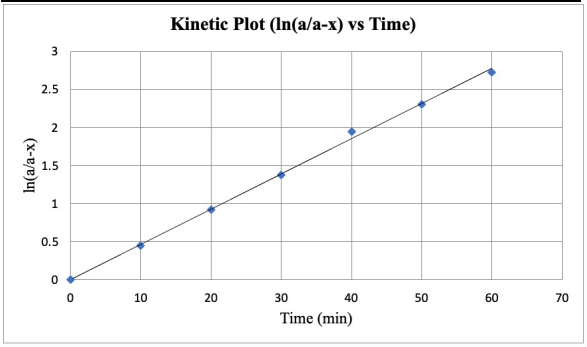

Figure 5: Kinetic Analysis for the Degradation of Dye

Higher slope values indicate faster degradation rates. The results are consistent with Langmuir–Hinshelwood kinetics observed in immobilized TiO_2 and polymer-supported photocatalysts [33–35].

FTIR Analysis: FTIR spectra of the effluent before treatment showed characteristic absorption peaks at:

- 1500-1600 cm^{-1} (–N=N– stretching of azo group),
- 1400-1500 cm^{-1} (C–N stretching), and
- 1150 cm^{-1} ($–SO_3^-$ symmetric stretching).

After photocatalysis, these peaks either disappeared or shifted to lower intensity, no peaks appeared between 1500-1600 cm^{-1} indicating breakdown of the aromatic structure and formation of intermediate oxidation products.

These changes confirm the successful oxidative cleavage of the azo linkage and ring-opening reactions.

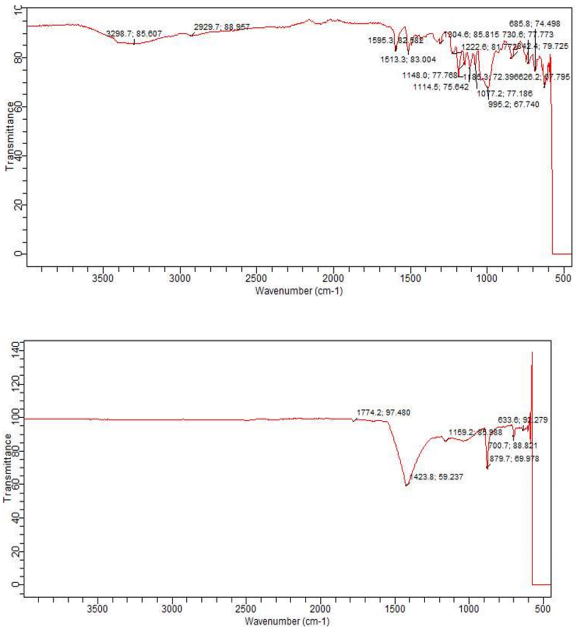

Figure 6: FTIR Spectra of Metanil Yellow Dye (a) before and (b) after photodegradation

COD and BOD Reduction: COD reduction from **785 mg L^{-1} to 62 mg L^{-1}** and BOD reduction from **220 mg L^{-1} to 35 mg L^{-1}** verified near-complete mineralization. This corresponds to **92.1% COD removal** and **84.1% BOD reduction**. Such decline demonstrates that Dowex-1×4-assisted photocatalysis not only decolorizes but also detoxifies the effluent.

Reusability of Catalyst: The Dowex-1×4 resin catalyst maintained 92–95% efficiency up to **five consecutive cycles** of reuse. Only a minor reduction (≈7%) was observed after the fifth run. The polymeric matrix prevented photocorrosion and leaching of metal ions, confirming the high mechanical and chemical stability of the system.

Comparative Evaluation: When compared with conventional semiconductor photocatalysts, the immobilized Dowex-1×4 system exhibited similar efficiency but with superior recovery and reusability. For example, TiO_2 powder achieves ~96% degradation but suffers 50% loss during recovery. Dowex-based catalysts provide a sustainable alternative with easier handling and negligible catalyst loss.

MECHANISM OF PHOTOCATALYTIC DEGRADATION

The degradation of Metanil Yellow under UV or sunlight primarily proceeds through electron excitation and the generation of highly reactive oxygen species, which subsequently attack and break down the dye molecules. The Dowex-1×4 resin used in this work functions as a photocatalyst after being impregnated with methylene blue (MB), a cationic and

photosensitive dye. During immobilization, MB molecules occupy the pores of the resin matrix.

Upon absorption of incident light, the MB molecules undergo photoexcitation. When photons strike the dye, electrons are promoted from the valence band (VB) to the conduction band (CB), causing a transition from the singlet state to the triplet state through inter-system crossing (ISC).

This excitation process triggers the formation of hydroxyl radicals ($^{\bullet}OH$) and superoxide ions (O_2^-) within the resin pores. These reactive species possess strong oxidative potential and play a crucial role in the photocatalytic breakdown of Metanil Yellow.

$$Dye + h\nu \longrightarrow Dye^{*S}$$

$$Dye^{*S} \xrightarrow{ISC} Dye^{*T}$$

$$MBIR + Dye^{*T} \rightarrow MBIR(e^-) + Dye^+$$

$$MBIR(e^-) + O_2 \rightarrow MBIR + O_2^-$$

$$Dye^+ + OH^- \rightarrow Dye + {}^{\bullet}OH$$

$$Dye/Dye^+ + {}^{\bullet}OH/\ O_2^- \rightarrow Product$$

MBIR = Methylene blue Immobilized Resin

CONCLUSION

This study demonstrates the successful application of **immobilized Dowex-1×4 resin** for the photocatalytic degradation of textile effluent containing Metanil Yellow dye. Key findings are as follows:

1. The optimized conditions (30 mg L^{-1} dye, 2.50 g catalyst, pH 7.5, 10.5 $mWcm^{-2}$ UV lamp) achieved **≈95% color removal**.
2. The process followed pseudo-first-order kinetics ($k = 0.046\ min^{-1}$).
3. COD and BOD reductions of 92% and 84% confirmed substantial mineralization.
4. The catalyst retained high efficiency (≥90%) even after five cycles.
5. FTIR results validated cleavage of azo bonds and formation of non-toxic oxidation products.

Hence, the **Dowex-1×4-assisted photocatalytic treatment** offers an economical, efficient, and eco-friendly solution for dye removal from textile wastewater, especially suitable for **arid and semi-arid industrial zones**.

ACKNOWLEDGEMENTS

The authors are grateful to the Department of Chemistry, Jai Narain Vyas University, Jodhpur, for providing laboratory facilities and to the staff of Basni Industrial Area for access to textile effluent samples.

REFERENCES

1. Akpan, U. G.; Hameed, B. H. Parameters affecting the photocatalytic degradation of dyes using TiO_2-based photocatalysts: a review. *J. Hazard. Mater.* **2009**, *170*, 520–529.
2. Herrmann, J. M. Heterogeneous photocatalysis: fundamentals and applications to the removal of various types of aqueous pollutants. *Catal. Today* **1999**, *53*, 115–129.
3. Chong, M. N.; Jin, B.; Chow, C. W. K.; Saint, C. Recent developments in photocatalytic water treatment technology: a review. *Water Res.* **2010**, *44*, 2997–3027.
4. Kaur, P.; Sud, D. Photocatalytic degradation of dyes using TiO_2: Effect of operational parameters. *Desalination Water Treat.* **2015**, *54*, 1720–1731.
5. Houas, A.; Lachheb, H.; Ksibi, M.; Elaloui, E.; Guillard, C.; Herrmann, J. M. Photocatalytic degradation pathway of methylene blue in water. *Appl. Catal. B* **2001**, *31*, 145–157.
6. Ahmad, R.; Kumar, R. Adsorptive and photocatalytic removal of textile dyes from water using TiO_2 nanoparticles: a comparative study. *J. Ind. Eng. Chem.* **2010**, *16*, 394–400.
7. Khataee, A. R.; Kasiri, M. B. Photocatalytic degradation of organic dyes in the presence of nanostructured titanium dioxide: influence of operational parameters. *J. Mol. Catal. A* **2010**, *328*, 8–26.
8. Natarajan, T. S.; Bajaj, H. C.; Tayade, R. J. Photocatalytic reactor configurations for water purification: overview and critical analysis. *Ind. Eng. Chem. Res.* **2018**, *57*, 272–295.
9. Rauf, M. A.; Ashraf, S. S. Fundamental principles and application of heterogeneous photocatalytic degradation of dyes in solution. *Chem. Eng. J.* **2009**, *151*, 10–18.
10. Selli, E.; Albanis, T. A. Photocatalytic degradation of azo dyes in aqueous TiO_2 dispersions. *Appl. Catal. B* **2002**, *38*, 91–105.
11. Fujishima, A.; Zhang, X.; Tryk, D. A. TiO_2 photocatalysis and related surface phenomena. *Surf. Sci. Rep.* **2008**, *63*, 515–582.

12. Jain, R.; Mathur, M.; Sikarwar, S.; Mittal, A. Removal of hazardous dye rhodamine B through photocatalytic and adsorption treatments. *J. Environ. Manage.* **2007**, *85*, 956–964.
13. Gupta, V. K.; Suhas. Application of low-cost adsorbents for dye removal – a review. *J. Environ. Manage.* **2009**, *90*, 2313–2342.
14. Linsebigler, A. L.; Lu, G.; Yates, J. T. Photocatalysis on TiO_2 surfaces: principles, mechanisms, and selected results. *Chem. Rev.* **1995**, *95*, 735–758.
15. Konstantinou, I. K.; Albanis, T. A. TiO_2-assisted photocatalytic degradation of azo dyes in aqueous solution: kinetic and mechanistic investigations. *Appl. Catal. B* **2004**, *49*, 1–14.
16. Devi, L. G.; Kumar, S. G. Visible light induced photocatalytic degradation of reactive dyes by N-doped TiO_2 nanocatalysts. *J. Mol. Catal. A* **2011**, *334*, 65–72.
17. Tamez, C.; Castillo, A.; Luna, R. A. Heterogeneous photocatalysis of textile effluents: advances and perspectives. *J. Photochem. Photobiol. C* **2019**, *41*, 100317.
18. Rahman, K. M.; Islam, M. A.; Haque, A. Degradation of textile dye by UV–TiO_2 photocatalysis. *Environ. Nanotechnol. Monit. Manage.* **2021**, *16*, 100492.
19. Kalra, S.; Chauhan, G. S. Ion-exchange resin-supported TiO_2 catalysts for photodegradation of dyes. *Polym. Degrad. Stab.* **2014**, *101*, 100–108.
20. Shaban, M.; El Sayed, A. M. Immobilization of TiO_2 nanoparticles on polymeric supports for improved photocatalytic performance. *J. Environ. Chem. Eng.* **2016**, *4*, 1340–1350.
21. Jothivenkatachalam, K.; Nithya, A.; Mohan, R. Degradation of textile effluents by immobilized photocatalysts. *Desalination Water Treat.* **2018**, *120*, 205–215.
22. Karthik, P.; Saravanan, R. Advanced polymer-supported catalysts for wastewater treatment. *Mater. Today Proc.* **2020**, *33*, 176–184.
23. Sharma, A.; Yadav, R.; Singh, P. Photocatalytic degradation of azo dyes by Dowex resin-immobilized nanoparticles. *J. Environ. Chem. Eng.* **2022**, *10*, 107192.
24. Patel, H. A.; Ray, J. R. Application of polymer-supported heterogeneous photocatalysts in industrial wastewater treatment. *Appl. Water Sci.* **2018**, *8*, 91.
25. Pal C.; Meena S. L.; Sharma A. Photocatalytic degradation of Bismarck Brown Y azo dye by using an immobilised photocatalyst and their reusability, *Current World Environment*, **2026**, 20(3), 1253–1264.
26. Yadav L.C.; Jaimini H.; Meena K.; Meena S. L. Photocatalytic degradation of Eriochrome Black-T dye by immobilized Dowex-1x8, *Research Journal of Chemistry and Environment*, **2023,** 27(10), 88–95.
27. Lin, Y.; Guo, X.; Chen, M. Photocatalytic mineralization of industrial dyes: influence of catalyst morphology. *Chemosphere* **2020**, *250*, 126217.
28. Singh, R.; Sharma, A. Photocatalytic oxidation pathways of reactive dyes: a comparative study. *Int. J. Environ. Sci. Technol.* **2021**, *18*, 2345–2356.
29. Kim, H.; Park, S. J. Advanced photocatalytic reactors for dye degradation. *Chem. Eng. J.* **2022**, *446*, 137238.
30. Chen, X.; Mao, S. S. Titanium dioxide nanomaterials: synthesis, properties, modifications, and applications. *Chem. Rev.* **2007**, *107*, 2891–2959.
31. Parida, K. M.; Naik, B.; Mohapatra, L. Photocatalytic degradation of organic pollutants under visible light irradiation. *J. Mater. Chem.* **2012**, *22*, 14701–14711.
32. Dong, F.; Li, Y.; Wang, Z.; Ho, W.-K. Enhanced visible light photocatalytic activity of polymer-based composites. *Appl. Catal. B* **2015**, *176–177*, 343–352.
33. Li, J.; Xu, L.; Zhang, H. Kinetic modeling of photocatalytic degradation of dyes in immobilized systems. *J. Photochem. Photobiol. A* **2019**, *384*, 112011.
34. Mehta, P.; Rani, A.; Singh, K. Langmuir–Hinshelwood kinetics of azo dye degradation using immobilized TiO_2 catalyst. *Indian J. Chem. Technol.* **2020**, *27*, 184–191.
35. Qureshi, Z.; Kiran, S.; Ahmad, T. Degradation of organic pollutants using polymer-supported TiO_2: a sustainable approach. *Environ. Sci. Pollut. Res.* **2021**, *28*, 53147–53158.